Citation: Molecular Therapy–Nucleic Acids (2012) 1, e32; doi:10.1038/mtna.2012.25

www.nature.com/mtna

Nonviral Direct Conversion of Primary Mouse Embryonic Fibroblasts to Neuronal Cells

Andrew F Adler[1], Christopher L Grigsby[1], Karina Kulangara[1], Hong Wang[2], Ryohei Yasuda[2,3] and Kam W Leong[1]

Transdifferentiation, where differentiated cells are reprogrammed into another lineage without going through an intermediate proliferative stem cell-like stage, is the next frontier of regenerative medicine. Wernig *et al.* first described the direct conversion of fibroblasts into functional induced neuronal cells (iNs). Subsequent reports of transdifferentiation into clinically relevant neuronal subtypes have further endorsed the prospect of autologous cell therapy for neurodegenerative disorders. So far, all published neuronal transdifferentiation protocols rely on lentiviruses, which likely precludes their clinical translation. Instead, we delivered plasmids encoding neuronal transcription factors (Brn2, Ascl1, Myt1l) to primary mouse embryonic fibroblasts with a bioreducible linear poly(amido amine). The low toxicity and high transfection efficiency of this gene carrier allowed repeated dosing to sustain high transgene expression levels. Serial 0.5 μg cm^{-2} doses of reprogramming factors delivered at 48-hour intervals produced up to 7.6% Tuj1^{+} (neuron-specific class III β-tubulin) cells, a subset of which expressed MAP2 (microtubule-associated protein 2), tau, and synaptophysin. A synapsin-red fluorescent protein (RFP) reporter helped to identify more mature, electrophysiologically active cells, with 24/26 patch-clamped RFP^{+} cells firing action potentials. Some non-virally induced neuronal cells (NiNs) were observed firing multiple and spontaneous action potentials. This study demonstrates the feasibility of nonviral neuronal transdifferentiation, and may be amenable to other transdifferentiation processes.

Molecular Therapy–Nucleic Acids (2012) **1,** e32; doi:10.1038/mtna.2012.25; advance online publication 10 July 2012.

Subject Category: Gene insertion, deletion & modification

Introduction

Neurodegenerative disorders, such as Alzheimer's disease (AD), Parkinson's disease (PD), Huntington's disease, and amyotrophic lateral sclerosis, lack effective treatment options.[1,2] These diseases are characterized by extensive cell death–loss of neurons in the neocortex and hippocampus in the case of AD, and loss of dopaminergic (DA) neurons in the substantia nigra in the case of PD. In AD and PD, cell-replacement therapy has been proposed as a more promising long-term alternative to pharmacologic intervention or high-frequency deep brain electrical stimulation, which lose efficacy as the diseases progress.[3] However, development of an appropriate therapeutic cell source has been a significant challenge. Although allogeneic transplantation of DA neurons from fetal ventral mesencephalic tissue into the striatum of PD patients has shown some clinical benefits,[4–7] the improvement is modest and overall results are mixed across several trials.[8,9] Societal concerns of using fetal tissue as a cell source and low yields of DA neurons from the tissue present additional challenges. Embryonic stem cells can be differentiated into functional neuronal cells,[10] and solve the problem of cell number, but safety and ethical issues remain. Induced pluripotent stem cells (iPSCs)[11] sidestep the ethical issues of embryonic stem cells, convert into DA neurons, and produce phenotypic recovery in an animal model of PD,[12] but the risk of teratoma formation persists.

In 2010, Wernig *et al.* succeeded in using three neuronal transcription factors (TFs)–Brn2, Ascl2, and Myt1l (BAM factors)–to convert mouse fibroblasts directly into functional neuronal cells,[13] referred to as induced neuronal cells (iNs). Human cells were converted subsequently with the addition of NeuroD1.[14] These iNs generate action potentials and form synapses when cocultured with primary cortical neurons or glia. Since its inception, the neuronal transdifferentiation field has expanded rapidly, with the identification of additional transcription factors that generate induced functional human dopaminergic neuronal cells (iDAs),[15–19] cholinergic motor neuronal cells (iMNs),[20] and the conversion of fibroblasts from patients with familial AD,[21] hepatocytes,[22] astrocytes,[19] as well as from cells infected with lentiviral miRNA/TF cocktails,[23,24] into functional neuronal cells.

When taken with lineage-tracing experiments that reveal iNs are not generated from and do not progress through an intermediate proliferative (cancerous) stem cell-like state,[20,22] the discovery that somatic cells can be robustly and directly transdifferentiated into many clinically relevant neuronal subtypes provides an exciting new cell source for autologous cell therapy against neurodegenerative diseases. So far all the neuronal transdifferentiation success has been achieved using lentiviral delivery strategies. These iNs are invaluable for neuronal disease recapitulation, drug discovery, and exploring the biology of transdifferentiation. However, the concern of genotoxic integration of therapeutic viral payloads into the host genome hinders the clinical translatability of

The first two authors contributed equally to this work.

[1]Department of Biomedical Engineering, Duke University, Durham, North Carolina, USA; [2]Department of Neurobiology, Duke University Medical Center, Durham, North Carolina, USA; [3]Howard Hughes Medical Institute, Duke University Medical Center, Durham, North Carolina, USA. Correspondence: Kam W Leong, 136 Hudson Hall, Box 90281, Durham, North Carolina 27708, USA. E-mail: kam.leong@duke.edu

Received 22 May 2012; revised 22 May 2012 ; accepted 22 May 2012

lentiviral iNs,[25] and encourages the search for efficient nonviral methods to generate these cells.

A critical finding of viral neuronal transdifferentiation studies is that the epigenetic program of the source cells is largely silenced in favor of a stable iN cell state,[22] which persists even when exogenous TF expression is discontinued. Endogenous neuronal TFs are activated and continue to be expressed after a relatively brief pulse of doxycycline (dox)-inducible ectopic transgene expression is shut down by dox withdrawal.[15,16] This, taken with the rapidness and high efficiency of iN generation, and the published success of nonviral iPSC generation,[26–30] suggested to us that neuronal transdifferentiation could be achieved with a clinically advantageous transient nonviral gene delivery strategy, which we demonstrate herein.

Results

Poly(CBA-ABOL)/DNA polyplexes mediate nontoxic and highly efficient transfection of a GFP-reporter plasmid in PMEFs

Of the three primary mouse embryonic fibroblast (PMEF) cell sources screened (PMEF-HL, PMEF-NL, and PMEF-CFL (Millipore, Billerica, MA)), we found PMEF-HLs to be the most efficiently transfected with p(CBA-ABOL)/DNA polyplexes (data not shown) and used them in all subsequent experiments. Fluorescence microscopy revealed that a 1.0 µg dose of pmax-GFP in p(CBA-ABOL) polyplexes produced high transfection efficiencies without noticeable toxicity (**Figure 1a**). Two microgram doses also gave high transfection efficiencies, with some visibly rounded and dead cells, and 4.0 µg was grossly toxic; 1.0 µg of pmax-GFP delivered

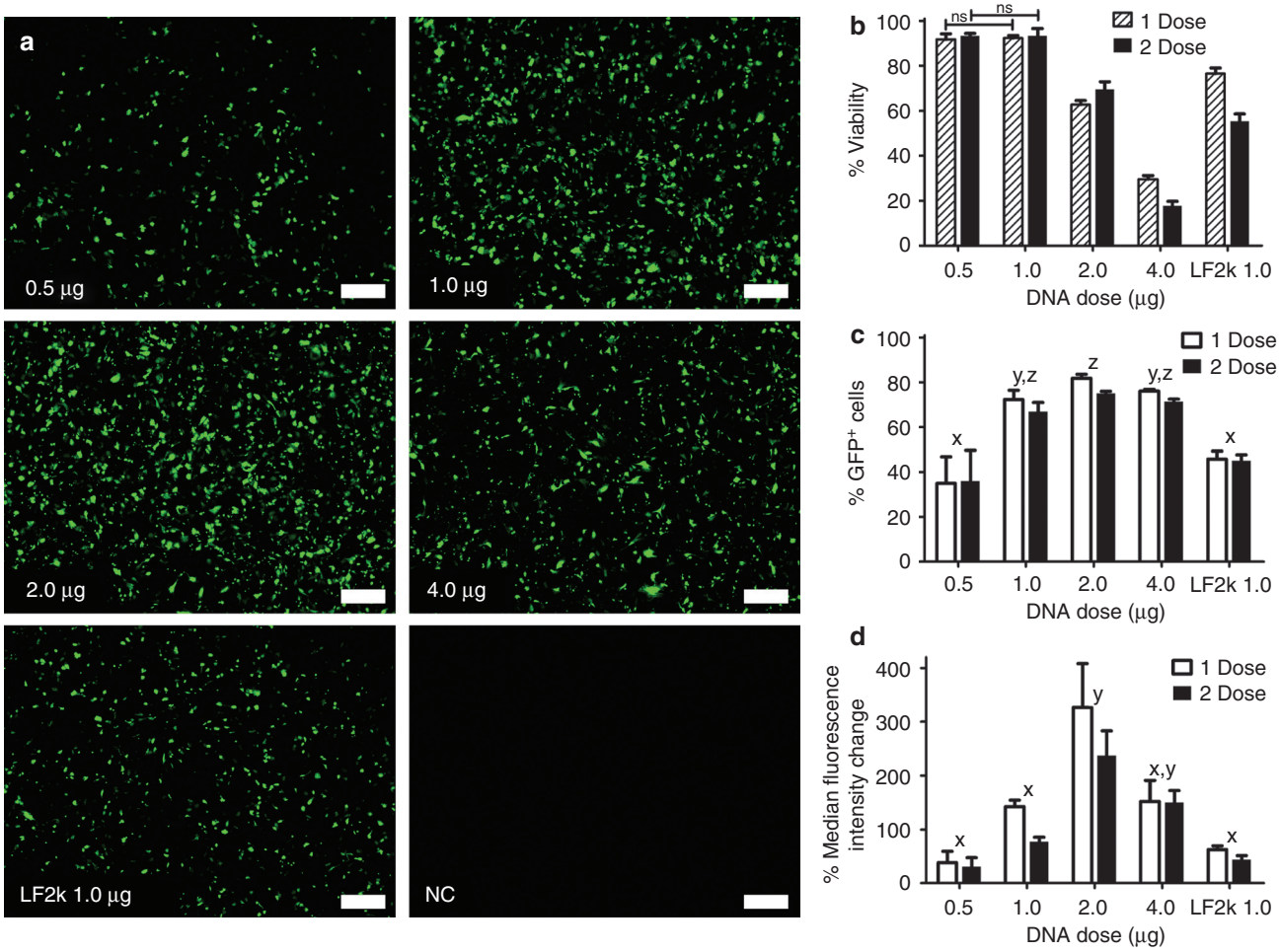

Figure 1 Optimization of nonviral GFP reporter plasmid transfection in PMEFs. (**a**) Fluorescence micrographs of PMEFs transfected with increasing doses of DNA in p(CBA-ABOL)/pmax-GFP polyplexes (Bar = 500 µm), with 1.0 µg of pmax-GFP delivered with Lipofectamine 2000 (LF2k) included for comparison. Images were taken 24 hours after transfection. (**b**) AlamarBlue toxicity assay multiplexed with (**c**) flow cytometric measurement of GFP transfection efficiency and (**d**) % median fluorescence intensity increase of GFP$^+$ cells compared to nonfluorescent control transfections for one and two doses of p(CBA-ABOL)/pmax-GFP polyplexes, assayed 24 hours after transfection; 1.0 µg of pmax-GFP delivered with LF2k is again included for comparison. Error bars represent mean ± SEM of three separate experiments performed in triplicate. Two-way ANOVA were performed with $P < 0.05$ considered significant. The main effect of DNA mass was significant in **b**–**d**, and the main effect of DNA dose number was significant in **b**. Letters (x,y,z) not shared between columns denote significant comparisons between DNA masses by Tukey post-hoc tests ($P < 0.05$) of one-way ANOVA across DNA masses, with data from one and two doses pooled in **c** and **d**, due to absence of a main effect of dose number by two-way ANOVA. All comparisons of viability (as shown in **b**) across DNA mass within a given dose number were significant, other than those between 0.5 and 1.0 µg pmax-GFP in p(CBA-ABOL) polyplexes (marked ns–not significant). ANOVA, analysis of variance; GFP, green fluorescent protein; NC, negative control; PMEF, primary mouse embryonic fibroblast.

with p(CBA-ABOL) transfected cells more efficiently than the same dose delivered with Lipofectamine 2000.

One and two doses of 1.0 µg pmax-GFP in p(CBA-ABOL) polyplexes were almost entirely nontoxic compared to untransfected controls, and a second transfection 48 hours later did not compound toxicity up to 2.0 µg (**Figure 1b**). Lipofectamine 2000 was significantly more toxic than p(CBA-ABOL) when delivering the same DNA dose, and its toxicity compounded with a second serial dose.

Flow cytometric quantification of green fluorescent protein (GFP) expression confirmed a high transfection efficiency for 1.0 and 2.0 µg pmax-GFP doses in p(CBA-ABOL) polyplexes, significantly higher than with Lipofectamine 2000 lipoplexes (**Figure 1c**). Further, a second dose maintained a high percentage of cells expressing GFP for an additional 2 days; without retransfection, the percentage of GFP$^+$ cells fell relatively by 15 and 28% for 1.0 and 2.0 µg pmax-GFP in p(CBA-ABOL) polyplexes, respectively (data not shown). Though 1.0 and 2.0 µg doses of pmax-GFP in p(CBA-ABOL) polyplexes elicited similar percentages of GFP$^+$ cells, the median fluorescence intensity (MFI) change of GFP$^+$ cells over nonfluorescent negative controls revealed that cells transfected with a 2.0 µg DNA dose had significantly higher GFP expression levels (**Figure 1d**).

Poly(CBA-ABOL)/DNA polyplexes elicit potent but transient expression of neuronal reprogramming factor mRNAs

An equimolar ratio of 1.0 µg pmax-BAM neuronal reprogramming factors in p(CBA-ABOL) polyplexes was delivered to PMEFs according to the scheme in (**Figure 2a**). Twenty-four hours after the initial transfection, each of the exogenous BAM factor transcripts were expressed at levels that were orders of magnitude higher than nontransfected PMEFs (**Figure 2b**). Ectopic expression of pmax-BAM factors diminished by approximately two orders of magnitude by day 10 of culture in N3 medium as the plasmids were silenced and/or degraded, for both one and three doses. Endogenous Ascl1 was activated in some cells by day 10 in N3 medium, as measured with primers targeted against an untranslated region of the endogenous transcript not present in the exogenous transcript. Tuj1 and MAP2 (microtubule-associated protein 2) transcripts were quantified but not detectably increased by transfection (data not shown).

Serial nonviral delivery of neuronal reprogramming factors generates Tuj1$^+$ cells efficiently

One dose of 1.0 µg pmax-BAM neuronal reprogramming factors in p(CBA-ABOL) polyplexes produced rare and isolated Tuj1$^+$ cells, whereas three and particularly five doses generated networks of Tuj1$^+$ cells showing varying degrees of neuronal and fibroblastic morphologies (**Figure 3a**). Neuron-like Tuj1$^+$ processes increased in length and complexity with increased culture time in N3 medium. Untransfected PMEFs were not reactive to antibodies against Tuj1. Automated microscopy and image analysis of large culture regions (**Figure 3b**) were used to quantify the efficiency of Tuj1$^+$ conversion relative to the number of PMEFs seeded (**Figure 3c**). Five doses produced significantly more Tuj1$^+$ cells than one or three doses. The increase in efficiency with dose is visually evident in the mosaic images of 24-well plates (**Figure 3b**).

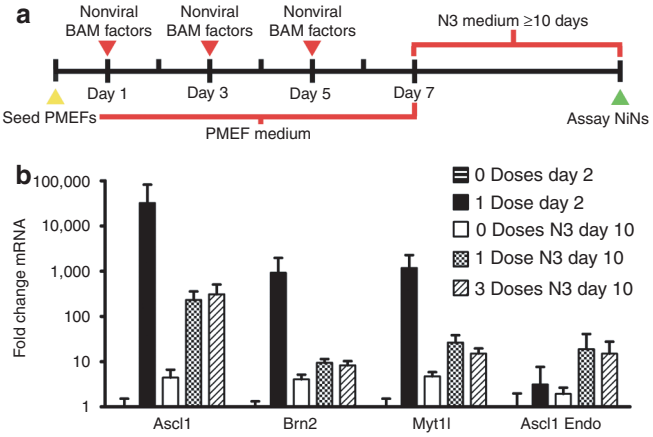

Figure 2 NiN generation schedule and resulting course of reprogramming factor gene expression. (**a**) NiN generation scheme. On day 0, PMEFs were seeded on TCPS wells or poly-D-lysine/laminin-coated glass coverslips in complete medium containing serum. Twenty-hour hours later, the first transfection was performed. Two to four additional doses were then administered every 48 hours. Beginning 48 hours after administration of the final dose, the cells were cultured for a minimum of 10 additional days before assay in serum-free N3 neural induction medium containing FGF2, which was replaced every 48 hours, or every 24 hours beyond day 10 in N3 for longer-term experiments. (**b**) Real-time comparative C_T RT-PCR of ectopic neuronal reprogramming factors (Ascl1, Brn2, Myt1l) and endogenous Ascl1 (Ascl1 Endo) mRNA expression. PMEFs were transfected with one or three doses of 1.0 µg pmax-BAM factors complexed with p(CBA-ABOL), and total mRNA was collected 24 hours after transfection (day 2) or after 10 days of culture in N3. Error bars represent the range of transcript produced by the SD about a mean C_T value ($n = 3$). FGF, fibroblast growth factor; mRNA, messenger RNA; NiN, non-virally induced neuronal cells; PMEF, primary mouse embryonic fibroblast; RT-PCR, reverse transcription-PCR; TCPS, tissue culture polystyrene.

Non-virally-induced neuronal cells express pan-neuronal cytoskeletal and synaptic proteins

After observing the feasibility of neuronal transdifferentiation using the BAM factors and Tuj1 staining, we added an additional set of plasmids to give the best chance of producing non-virally induced neuronal cells (NiNs) with active membrane properties. The cytomegalovirus (CMV) promoter is generally inactive in cortical neurons,[31] and it is not known if or at what point this silencing could occur during neuronal transdifferentiation. We therefore added a parallel plasmid cocktail with serial transfections of 2.0 µg pUNO-AM/pmax-B factors, which utilize the EF1α/HTLV promoter for Ascl1 and Myt1l expression instead of the CMV promoter in pmax-BAM plasmids, and would potentially take advantage of increased expression levels with 2.0 µg of plasmid compared to 1.0 µg.

Given the increased heterogeneity in maturity and completeness of NiNs compared to conventional iNs, we expected that upstream markers of neurogenesis, such as tau[13] or MAP2 promoter activity,[19] would likely be less useful in NiNs for predicting active membrane properties. Accordingly, we transduced NiNs with a lentiviral reporter driving expression of RFP under the control of the highly neuron-specific synapsin I promoter,[32,33] in order to help us identify the most mature NiNs for electrophysiological characterization. This lentivirus may have a natural tropism for excitatory cortical neurons,[34] which are similar to the predominant subtype generated by ectopic BAM expression in PMEFs.[13]

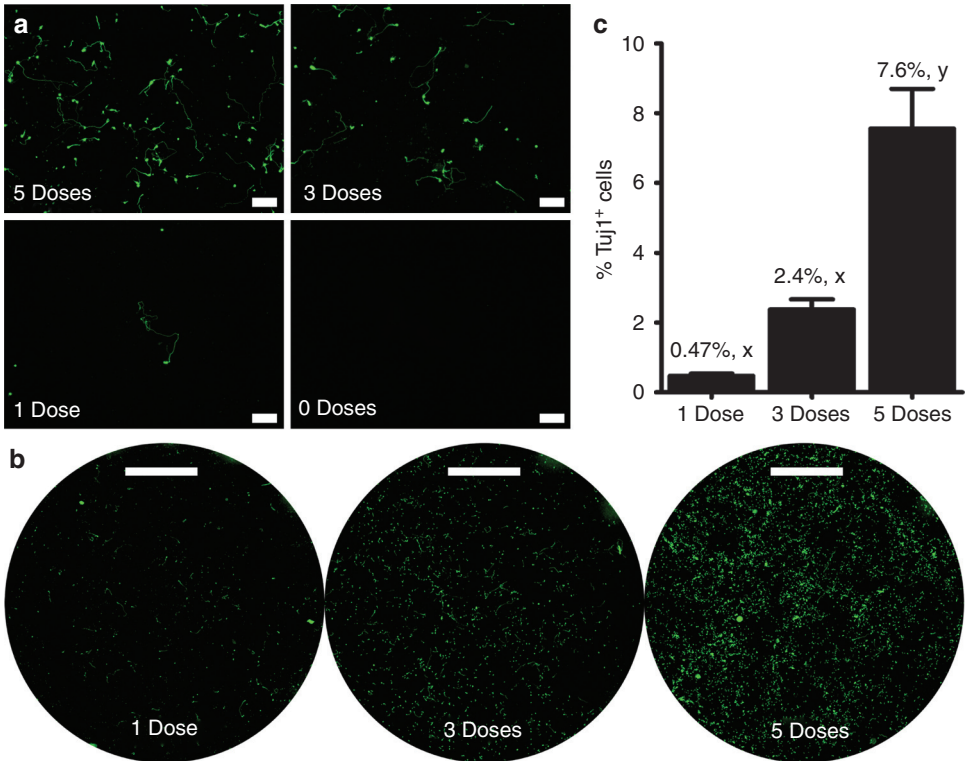

Figure 3 Tuj1 expression induced in cells transfected with multiple doses of reprogramming factor plasmids. (**a**) Tuj1 stain of cells transfected with one to five doses of 1.0 µg pmax-BAM factors in p(CBA-ABOL) polyplexes after a minimum of 14 days in N3 medium following transfection. Bar = 200 µm. (**b**) Large mosaic images of the entire culture area (Bar = 2.5 mm) acquired for image analysis-based quantification of the number of Tuj1+ cells normalized to the number of PMEFs seeded (**c**), after a minimum of 10 days in N3 following transfection. Letters (x,y) not shared between columns denote significant comparisons by Tukey post-hoc tests of a one-way ANOVA ($P < 0.05$). Error bars represent the mean ± SEM of three separate experiments performed in triplicate. ANOVA, analysis of variance; PMEF, primary mouse embryonic fibroblast.

Distal enrichment of tau (**Figure 4**, top row), characteristic of neurons, was visible for a subset of Tuj1+ cells (center and right panels). Tuj1+ cells with fibroblastic morphologies were not tau+ (red cells, left panel). Tuj1+ cells with neuronal morphology were also reactive to MAP2 antibodies (second row). Synaptophysin punctae were visible in a subset of Tuj1+ cells, a protein characteristic of synaptic vesicles (third row). Synapsin-RFP was also visible in long, branching processes. Synapsin-RFP+ cells were less common than any of those detected by immunofluorescence. Though comparatively uncommon, synapsin-RFP+ processes were present at sufficient densities and lengths to intersect with neighboring cells (fourth row), particularly for those transfected with the pUNO-AM/pmax-B cocktail (right panel). Approximately 0.1–1% of Tuj1+ cells were also synapsin-RFP+ for three doses of 1.0 µg pmax-BAM factors. This is significantly less efficient than our lentiviral derivation of iNs using the same TFs and PMEF source, with 66% synapsin-RFP+ cells generated from those plated, as detected by fluorescence-activated cell sorting (data not shown).

NiNs with synapsin I promoter activity are electrophysiologically active and complex

The presence of synapsin-RFP in long processes of NiNs was used to identify cells for electrophysiological recording; 12/13 synapsin-RFP+ cells produced with three doses of 1.0 µg pmax-BAM factors fired single action potentials in response to depolarizing current injection as shown in (**Figure 5a,b**). These cells had an average resting membrane potential of –46.3 ± 2.2 mV (mean ± SEM, $n = 12$), and an average input resistance of 1.7 ± 0.3 GΩ (mean ± SEM, $n = 11$); 12/13 synapsin-RFP+ cells produced with three doses of 2.0 µg pUNO-AM/pmax-B factors fired at least one action potential in response to depolarizing current injection. Further, 5/13 of these cells fired multiple action potentials as shown in (**Figure 5c,d**), and 7/13 fired single action potentials. One cell was observed firing spontaneous trains of action potentials (**Figure 5d**, 0 pA), and rebound action potentials were also recorded (**Figure 5c,d**). These cells had an average resting membrane potential of –41.7 ± 2.4 mV (mean ± SEM, $n = 12$), and an average input resistance of 1.5 ± 0.2 GΩ (mean ± SEM, $n = 12$). Results are for recordings with freely fluctuating resting membrane potentials, though maintaining the cells at approximately –65 mV with holding current between recordings did occasionally result in more clearly defined trains of action potentials. Qualitatively, we observed that cells firing trains of action potentials tended to have larger somas and expressed synapsin-RFP more intensely than those firing only once.

Discussion

Our aim in this study was to demonstrate direct neuronal transdifferentiation without viral delivery of TFs, in an effort to bring this exciting new field one step closer to

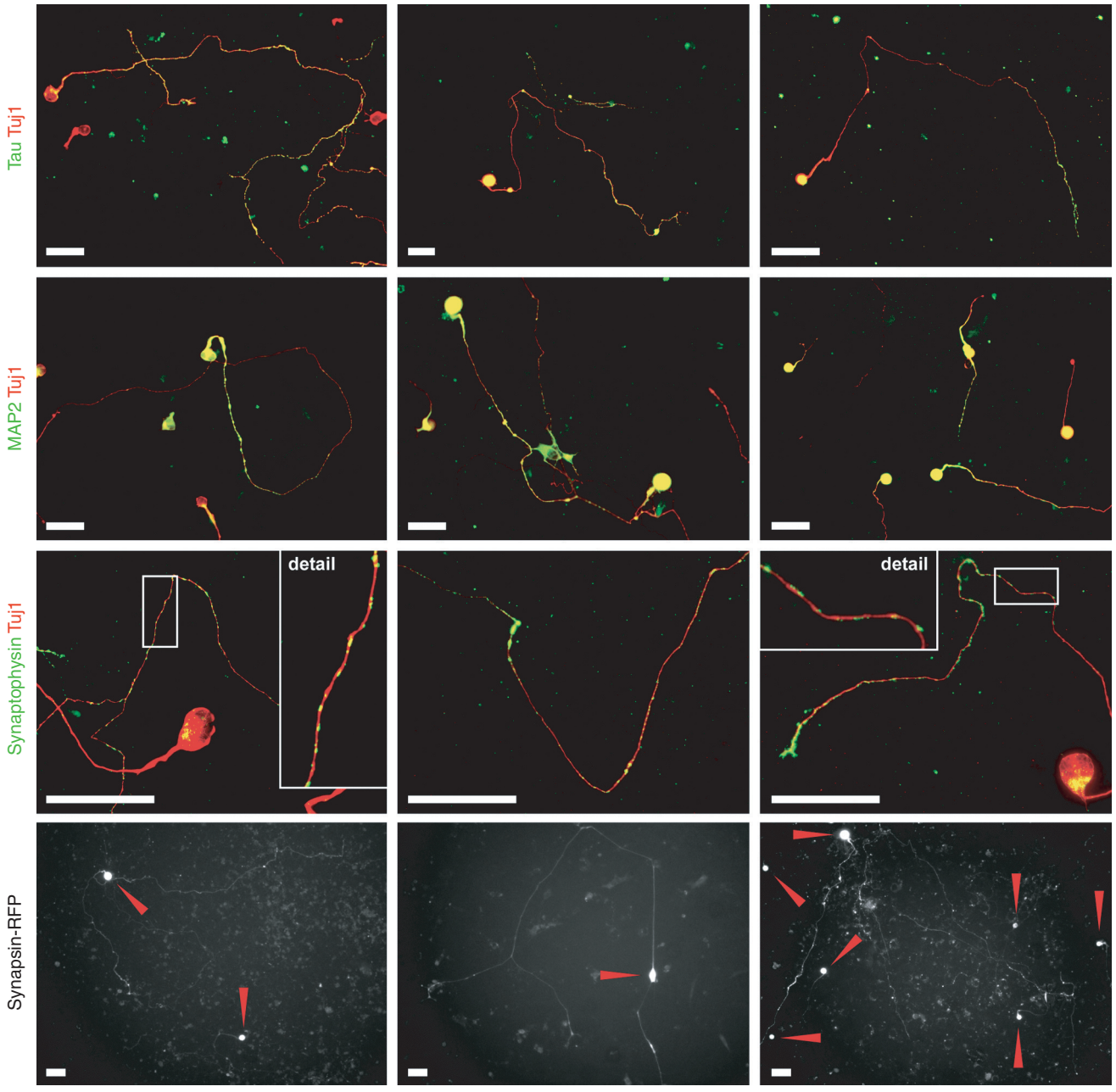

Figure 4 Immunofluorochemistry and synapsin reporter activity in NiNs generated with p(CBA-ABOL)/DNA polyplexes. All bars are 50 µm. Tau stain (first row): three doses of 1.0 µg pmax-BAM factors, ≥10 days in N3 medium, on TCPS. MAP2 stain (second row): three doses of 1.0 µg pmax-BAM factors (left panel), or 2.0 µg pUNO-AM/pmax-B factors (center and right panels), 16 days in N3, on poly-D-lysine/laminin-coated coverslips. Synaptophysin stain (third row): five (left and center panels) or three (right panel) doses of 1.0 µg pmax-BAM factors, 17 days in N3, on PDL/laminin-coated coverslips. Expression of RFP under control of the synapsin promoter (fourth row): three doses of 1.0 µg pmax-BAM factors (left and center panels), or 2.0 µg pUNO-AM/pmax-B factors (right panel), ≥10 days in N3, on PDL/laminin-coated coverslips. Synapsin-RFP images have not been false-colored red, in order to maximize visual contrast for thin cellular processes. Arrows indicate synapsin-RFP$^+$ cell bodies. NiN, non-virally induced neuronal cell; RFP, red fluorescent protein; TCPS, tissue culture polystyrene.

clinical translation. We hypothesized that multiple doses of reprogramming factors would be required to generate NiNs efficiently. Predicting that nonviral transdifferentiation would be less efficient than the viral systems, we elected to use PMEFs as a starting material; PMEFs are putatively the somatic cell type most susceptible to neuronal transdifferentiation.[13,22]

We used the three neuronal reprogramming factors Brn2, Ascl1, and Myt1l (BAM) in separate nonviral plasmids. Accordingly, we expect the proportion of cells that receive and express all three transgenes to be lower than that of those expressing only one or two.[35] The fraction of cells coexpressing all three can be roughly calculated by considering the fraction of cells positive for a single reporter, and raising

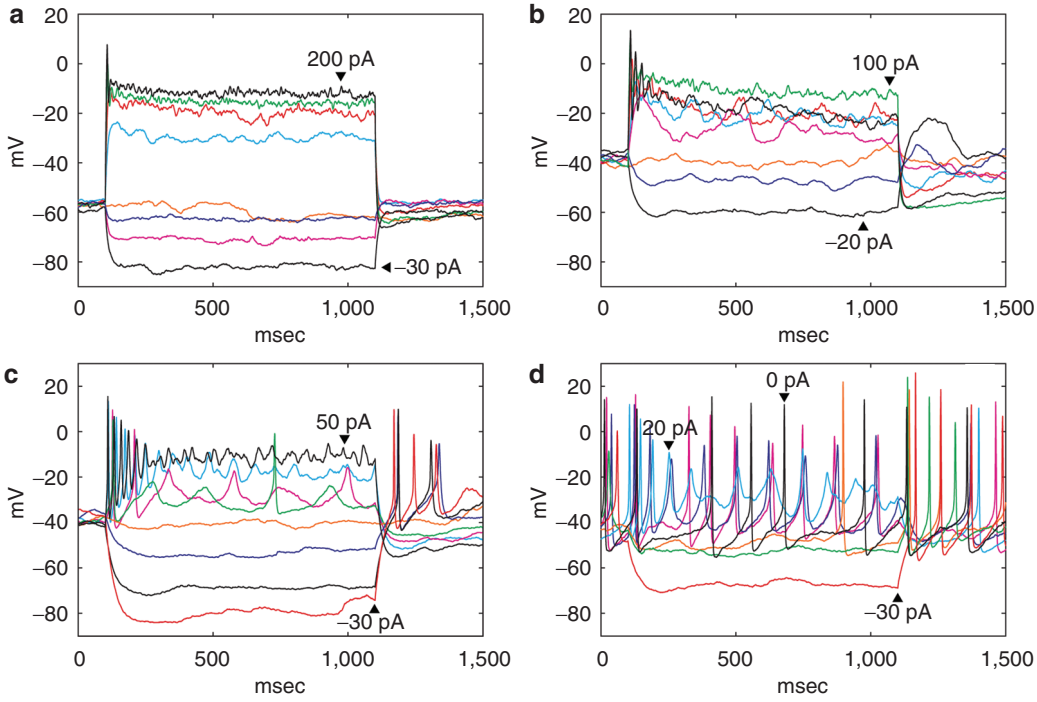

Figure 5 Current clamp in the whole-cell configuration of synapsin-RFP⁺ NiNs generated with p(CBA-ABOL)/DNA polyplexes. (**a**,**b**) Traces of cells that received three doses of 1.0 µg pmax-BAM factors, after 16–17 days of culture in N3 medium, on poly-D-lysine/laminin-coated coverslips. (**c**,**d**) Traces of cells that received three doses of 2.0 µg pUNO-AM/pmax-B factors, on day 12 of culture in N3, on PDL/laminin-coated coverslips. NiN, non-virally induced neuronal cell; RFP, red fluorescent protein.

it to the power *n* = number of transgenes that must be coexpressed. This worst-case is mitigated somewhat by our inclusion of all three factors in the same polyplexes, such that they are co-endocytosed, but it is helpful to realize the large benefit high transfection efficiencies have on coexpression of multiple plasmids. For example, if a population is transfected with 20% efficiency for one of three separate genes, ~100% × $(0.2)^3$ = 0.8% will be positive for all three factors. An 80% transfection efficiency would produce 100% × $(0.8)^3$ = 51% triple-positive cells (a 60-fold increase). This is particularly important when serial dosing is required, which will compound the effect.

Previous reports have clearly demonstrated the importance of coexpression of all three BAM factors to produce iNs with mature electrophysiological phenotypes,[13] which we expected to occur for a subset of cells transfected with our system. Improvement in transfection efficiency should result in nonlinear improvement in the appearance of NiNs firing multiple action potentials. p(CBA-ABOL) is a highly efficient and nontoxic gene carrier that is rapidly degraded upon delivery to the reducing intracellular environment, for favorable unpacking of the polyplex.[36] In our hands, p(CBA-ABOL) outperforms most commercially available transfection reagents *in vitro*. The high efficiency and low cytotoxicity of this gene carrier is key to the success of the current study, as serial multiple-plasmid transfections are helpful for efficient NiN generation.

Optimization of PMEF transfection demonstrated that p(CBA-ABOL) polyplexes are nontoxic for doses that elicit very efficient transgene expression (**Figure 1b,c**). A 2.0 µg dose was identified as the highest dose suitable for serial delivery without toxicity concern. p(CBA-ABOL) is more efficient and less toxic than Lipofectamine 2000, which we deemed to be inappropriate for multiple dose delivery due to its compounding toxicity. We have previously observed a sharp threshold for p(CBA-ABOL) efficacy, near 0.5 µg. To avoid inconsistent transfection and significant toxicity, our operating range for these experiments was therefore 1.0–2.0 µg. Maintenance of high transfection efficiencies upon administration of a second dose is likely due to retransfection of fibroblasts silencing the transgene(s), as well as from transfection of newly divided PMEFs replacing those lost to toxicity. The increase in expression levels for 2.0 µg compared to 1.0 µg (**Figure 1d**) is important, particularly if there is a threshold level of transcription factor that must be expressed in a given cell to "pioneer" heterochromatin or to outcompete a fibroblastic epigenetic program to "throw the switch" on transdifferentiation.[37,38]

Using 1.0 µg of pmax-BAM factors, we observed robust ectopic expression of BAM factor messenger RNA (mRNA) (**Figure 2b**) and endogenous activation of Ascl1, but no upregulation of MAP2 or Tuj1 mRNA. However, the presence of Tuj1 and MAP2 at the protein level (**Figure 4**) highlights the necessity of fluorescence-activated cell sorting enrichment *via* a neuronal reporter or single-cell PCR[39] when attempting to analyze iN mRNA amidst a background of unconverted cells. The exogenous BAM factors were silenced to a large extent by day 10 in N3 medium, supporting the use of this technique as a transient expression system. Further transgene silencing is expected to continue with increased time in culture. Integration of nonviral DNA vectors occurs rarely,[26,28,40] but direct transdifferentiation is superior to iPSC systems in this regard in that sporadic BAM factor reactivation would lead to growth arrest, rather than tumorigenic proliferation.

The morphological heterogeneity of Tuj1+ cells generated by our technique (**Figure 3a**) is further confirmation of Tuj1+ as an early or promiscuous marker of induced neurogenesis.[38] However, a subset of these cells have more complete neuronal morphologies and phenotypes, and increasing the number of Tuj1+ cells is therefore likely predictive of an increased number of more mature NiNs at downstream analysis points, and is hence useful for screening experiments without the use of transgenic neuronal reporter cells. The nonlinear improvement in the efficiency of Tuj1 induction with an increasing number of serial transfections (**Figure 3b,c**) may be a consequence of the retransfection of individual cells that did not initially express sufficient transcription factor to surpass the threshold required for transdifferentiation, and also of the potential continued proliferation and subsequent transfection of unconverted PMEFs. It seems likely that additional doses could further increase the efficiency of Tuj1+ cell generation.

In accordance with the mixture of fibroblastic and neuron-like Tuj1+ cell morphologies, immunofluorochemistry revealed a similar heterogeneity in the expression of pan-neuronal markers (**Figure 4**). Delivering separate transcription factors with both pmax-BAM and pUNO-AM/pmax-B plasmids resulted in some more mature NiNs that expressed MAP2, distal tau enrichment, Tuj1, synaptophysin punctae, and had synapsin promoter activity, as well as some less mature cells that expressed a subset of these markers. These less complete neuron-like cells may have received an inappropriate timing, amount, or mixture of transcription factors, or may have been on their way to becoming fully reprogrammed NiNs. Though heterogeneous on the population level, the presence of non-virally induced markers of maturing neuronal cells (synapsin promoter activity, synaptophysin punctae) forecasted the neuron-like electrophysiological properties of these cells.

The synapsin-RFP reporter was excellent at predicting which cells would fire action potentials, with 24/26 patched cells firing (**Figure 5**). These cells had heterogeneous resting membrane potentials, action potential thresholds, action potential amplitudes, and number of action potentials. We observed action potentials after hyperpolarization (**Figure 5c**), and spontaneous action potentials (**Figure 5d**) for NiNs generated with 2.0 µg pUNO-AM/pmax-B factors. These heterogeneous active membrane properties are again indicative of the myriad combinations of BAM factors the cells receive during nonviral transdifferentiation, producing NiNs in different stages of maturity and completion.

NiNs generated with pmax-BAM factors were electrophysiologically similar to iNs produced with lentiviral transduction of Ascl1 only.[13] Ascl1 is the only member of the BAM factors that is able to generate cells with active membrane responses on its own. As such, if a population of cells tends to receive a supra-threshold dose of only one of the transcription factors, Ascl1 cells may be the only ones detected as synapsin-RFP+. pmax-BAM vectors may be silenced before an expression time has been reached that is sufficient for Brn2 or Myt1l to act, or the more prevalent pmax-Ascl1 transcript may have out-competed pmax-Brn2 and -Myt1l for translational machinery.[41] The 2.0 µg dose of pUNO-AM/pmax-B factors may have elicited higher (or more balanced) overall expression levels compared to 1.0 µg of pmax-BAM factors. The use of separate plasmids would allow simple alteration of BAM plasmid ratios to correct such an imbalance, if necessary.

These results are the first example of nonviral direct neuronal transdifferentiation. We believe this method will prove useful in the nonviral production of subtype-specific neuronal cells, as well as provide an accessible means of generating iNs without lentivirus. Lentiviral protocols have demonstrated that adult human cells may be intrinsically more resistant to neuronal transdifferentiation than are embryonic mouse cells, and as such our nonviral approach can benefit from further increases in efficiency as it is deployed in human cells. The effectiveness of the nonviral technique will undoubtedly improve as polycistronic vectors for iN generation become more readily available,[19,21] which, by removing redundant plasmid backbone sequences, will increase the effective dose of each factor, and ensure coexpression of all factors in transfected cells. Work is underway to modify these polycistronic vectors for nonviral use in adult human cells to generate human NiNs at a sufficient density to allow study of their synaptic properties and their accordant designation as "fully-mature" iNs,[38] and to achieve a therapeutic efficiency. The recent discovery that small molecules can greatly boost the efficiency of neuronal transdifferentiation is also expected to help reach this goal.[42] Subtype-specific human NiN generation will likely require a longer pulse of ectopic expression,[16] which will further rely on the unique non-toxicity of p(CBA-ABOL). Though the non-integrative requirement for *ex vivo* generation of nonproliferative therapeutic NiNs is relaxed compared to iPSCs, mRNA vectors will be of interest, but may need to be delivered even more frequently to maintain sufficient expression levels.

When the scalability of p(CBA-ABOL) synthesis is taken together with successful demonstration of iMN[20] and iDA[16] engraftment and iDA functional improvement in animal models of PD,[17,18] the goal of cell-replacement therapies using NiNs for a number of neurodegenerative diseases seems attainable. For example, if this nonviral method were modified with a different TF cocktail to produce functional dopaminergic neurons with five 1 µg doses at a 7.5% efficiency, only ~0.5% of a typical p(CBA-ABOL) synthesis and ~1% of a Plasma Giga Kit product (QIAGEN, Hilden, Germany) would be required to generate enough neurons to produce phenotype correction in a Parkinsonian rat.[17] The benefit-to-risk ratio of neuroprotective AAV gene therapy to combat PD is already deemed high enough to warrant clinical trials,[43] so the introduction of an ethically and technically viable autologous nonviral source of neuronal cells should be of great therapeutic value. The reduced risk of insertion mutagenesis with this nonviral approach should further lower the entry barrier for a variety of neurological diseases. Further, our demonstration of NiN generation is suggestive of the feasibility of other forms of nonviral interlineage transdifferentiation.[44–48]

Materials and methods

Molecular cloning and plasmid purification. The reporter vectors pmax-GFP (3486 bp; Amaxa, Cologne, Germany) and VR1255C (6,413 bp; Vical, San Diego, CA), which respectively express GFP and luciferase under control of

the CMV promoter, were used for flow cytometric measurement of transfection efficiency. pmax-Brn2 (4,154 bp), pmax-Ascl1 (3,497 bp), and pmax-Myt1l (6,359 bp), which express the mouse transcription factors Brn2, Ascl1, and Myt1l, respectively, under control of the CMV promoter, were generated by first excising the GFP coding sequence from pmax-GFP with SacI digestion, blunting by DNA polymerase I Klenow fragment, NheI-HF digestion (NEB, Ipswich, MA), and gel extraction (QIAquick Gel Extraction Kit; QIAGEN, Hilden, Germany). Then, Brn2, Ascl1, and Myt1l inserts were prepared by digestion of the lentiviral vectors Tet-O-FUW-Brn2 (Addgene 27151), Tet-O-FUW-Ascl1 (Addgene 27150), and Tet-O-FUW-Myt1l (Addgene 27152) with EcoRV and NheI-HF (NEB) and gel extraction, and were subsequently ligated into the empty pmax vector with T4 DNA ligase (NEB). When used together, these three plasmids are abbreviated as pmax-BAM. pUNO1-mAscl1 (3,892 bp; InvivoGen, San Diego, CA) and pUNO1-mMyt1lb (6,744 bp; InvivoGen), expressing mouse Ascl1 and Myt1l under control of the EF1α/HTLV promoter, were used in conjunction with pmax-Brn2, and when used together are abbreviated as pUNO-AM/pmax-B. Plasmids were propagated in *Escherichia coli* DH5α (Invitrogen, Carlsbad, CA) and purified with EndoFree Plasmid Mega and Maxi kits (QIAGEN). Plasmid DNA concentrations were quantified by measurement of absorbance at 260 nm with a NanoDrop ND-1000 Spectrophotometer (Thermo Scientific, Waltham, MA).

Production and purification of lentiviral synapsin reporter. Stbl3 bacteria (Invitrogen) were transformed with pLV-hSyn-RFP[34] (Addgene 22909) according to the manufacturer's protocol. Plasmid DNA was propagated and purified using the EndoFree Maxiprep kit (QIAGEN). For the lentiviral production, HEK293T cells were seeded in 75 cm^2 dishes, cultured in DMEM (Invitrogen) containing 10% Premium Select FBS (Altanta Biologicals, Lawrenceville, GA) and 1% penicillin-streptomycin (Invitrogen), and were transfected by the calcium phosphate technique with the following plasmids: 16.9 µg of pMD2.G (Addgene plasmid 12259), 31.3 µg of psPAX2 (Addgene plasmid 12260), and 48.2 µg of pLV-hSyn-RFP. The medium was changed after 14 hours. Seventy-two hours after transfection, the medium was collected in 50 ml tubes, centrifuged, and filtered through a 0.45 µm filter to remove cell and membrane debris. The supernatant was then concentrated to 100× in Amicon Ultra centrifugal filter tubes (Millipore) and the concentrated virus was stored at −80 °C. PMEFs in 2 cm^2 wells were infected with 1 µl of 100× viral concentrate in PMEF medium 5 days before patch clamping.

Poly(CBA-ABOL) synthesis and polyplex formation. Poly(CBA-ABOL) was synthesized by Michael polyaddition of 3.67 g N,N-cystaminebisacrylamide (CBA) (Polysciences, Warrington, PA) and 1.26 g 4-amino-1-butanol (ABOL) (Sigma-Aldrich, St Louis, MO) as described by Lin *et al.*[36] The reaction product was purified by dialysis (3.5 kDa cutoff) in acidic deionized water (pH 4) and then lyophilized. The polymer was collected in its HCl-salt form (1.63 g, 33% yield), and its structure validated by ^{1}H NMR (in D_2O) on a Varian Mercury 300 MHz NMR Spectrometer (Agilent, Palo Alto, CA). p(CBA-ABOL)/DNA nanocomplexes (polyplexes) were synthesized at a polymer:DNA mass ratio of 45:1, which was selected based on a preliminary optimization of GFP expression in PMEFs (data not shown). Polyplexes were prepared by adding a HEPES buffer solution (20 mmol/l HEPES, 5 wt % glucose, pH 7.4) of p(CBA-ABOL) (900 µg/ml) to a HEPES buffer solution (20 mmol/l HEPES, 5 wt % glucose, pH 7.4) of plasmid DNA (75 µg/ml), followed immediately by vortexing for 20 seconds. Reaction sizes ranged from 5 to 15 µg of plasmid DNA. Average p(CBA-ABOL)/pmax-BAM polyplex diameter was 102.5 ± 3.7 nm, and zeta potential was +23.5 ± 1.5 mV (mean ± SEM, $n = 3$), as measured with a Zetasizer Nano ZS (Malvern Instruments, Malvern, UK).

Cell culture and transfection. A total of 40,000 cells (80,000 cells) passage six (eight) PMEF-HLs (Millipore) were seeded per well in 24-well TCPS plates (BD, Franklin Lakes, NJ) at 37 °C and 5% CO_2 in complete PMEF medium: Dulbecco's Modified Eagle's Medium with 4.5 g/l glucose (GIBCO 11960-044) (Invitrogen), 10% Premium Select FBS (Atlanta Biologicals), 25 µg ml^{-1} gentamicin (Invitrogen), and 1× GlutaMAX, nonessential amino acids, sodium pyruvate, and β-mercaptoethanol (Invitrogen). In the case of electrophysiology and most immunofluorochemistry experiments, 12 mm BD BioCoat poly-D-lysine/laminin-coated glass coverslips were placed in the bottom of TCPS wells before cell seeding. Twenty-four hours after seeding, PMEFs were transfected with either: reporter plasmids for flow cytometry, or pmax-BAM or pUNO-AM/pmax-B plasmid cocktails for induced neuronal transdifferentiation. BAM factor plasmids were delivered at an equimolar ratio in all cases. A 2:1 ratio of Lipofectamine 2000 (Invitrogen) volume (µl) to DNA mass (µg) was used for flow cytometry experiments, in accordance with the manufacturer's protocol. All transfections were carried out in serum- and antibiotic-free OptiMEM (Invitrogen). OptiMEM was replaced with complete PMEF medium 4 hours after the onset of transfection. Serial transfections for neuronal transdifferentiation proceeded as depicted in (**Figure 2a**). Forty-eight hours after the final transfection was completed, PMEF medium was replaced with N3 neural induction medium containing: DMEM/F-12 (Invitrogen), 25 µg ml^{-1} bovine insulin (Gemini Bio-Products, West Sacramento, CA), 50 µg ml^{-1} human apo-transferrin, 30 nmol/l sodium selenite, 20 nmol/l progesterone, 100 µmol/l putrescine (Sigma-Aldrich), 10 ng ml^{-1} human bFGF2 (Stemgent, Cambridge, MA), and 25 µg ml^{-1} gentamicin (Invitrogen).

Viability assay. The quantification of PMEF viability following transfection was duplexed with flow cytomety experiments. Twenty-four hours after the onset of the final transfection with pmax-GFP, cells were incubated for 4 hours with fresh PMEF medium containing alamarBlue (Invitrogen) in accordance with the manufacturer's protocol. Metabolic reduction of alamarBlue was monitored at 570 nm/590 nm excitation/emission using a BMG Labtech FLUOStar Optima plate reader (BMG Labtech, Ortenberg, Germany). AlamarBlue-containing medium was then removed, and the cells were prepared for flow cytometry.

Flow cytometry. Twenty-four hours after completion of the final transfection with pmax-GFP, PMEFs were washed briefly with phosphate-buffered saline (PBS) without Ca^{2+} and Mg^{2+} (Mediatech, Washington, DC), and released from TCPS surfaces with 0.25% Trypsin-EDTA (Invitrogen). The trypsin was inactivated with serum-containing medium and the cells were centrifuged at 4 °C, resuspended in ice-cold PBS, centrifuged again, and resuspended in PBS containing 1% paraformaldehyde (EMS, Hatfield, PA). Cells were then filtered through 40 µm nylon cell strainers (BD) and analyzed with a BD FACSCanto II flow cytometer. PMEFs transfected with the nonfluorescent VR1255C plasmid served as negative controls for each equivalent pmax-GFP dose, with gates set such that 1% of these cells were considered GFP^+. The recorded median fluorescent intensities of GFP^+ cells (MFI_{GFP}) were linearized according to an assumption of ideal logarithmic amplifier behavior, and normalized by the median fluorescent intensity of negative control cells (MFI_{NC}) to calculate the reported % MFI change: $100\% \times (MFI_{GFP} - MFI_{NC})/MFI_{NC}$.

Real-time reverse transcription-PCR. Comparative C_T real-time reverse transcription-PCR was performed in 20 µl reactions using the QuantiTect SYBR Green RT-PCR Kit (QIAGEN) with 10 ng of starting mRNA isolated with RNeasy and QIAshredder kits (QIAGEN) from cells transfected with pmax-BAM factors. mRNA concentrations were quantified with a NanoDrop ND-1000 Spectrophotometer (Thermo Scientific). PCR proceeded for 40 cycles in an ABI 7300 Real-Time PCR System (Applied Biosystems, Carlsbad, CA). Target mRNA levels were normalized to endogenous GAPDH references, and presented as a fold-change increase relative to expression levels from untransfected PMEF mRNA collected 48 hours after seeding. Correct reverse transcription-PCR target amplicon lengths for exogenous pmax-BAM factors were verified with gel electrophoresis in a separate experiment. Primers (IDT, Coralville, Iowa) were as follows: Ascl1 forward (GCTGCAAACGCCGGCTCAAC); Ascl1 reverse (GCGGATGTACTCGACCGCCG); Ascl1 endo forward (TGGCGGGTTCTCCGGTCTCGT); Ascl1 endo reverse (TCCCCATTTGACGTCGTTGGCGA); Brn2 forward (CCATCGTACATGCCGAGCCGC); Brn2 reverse (GCGCGGTGATCCACTGGTGAG); Myt1l forward (CGGG TGTGATGGAACCGGCC); Myt1l reverse (GCCCTGTGCAG CCTGGAGTG); GAPDH forward (ACGGCCGCATCTTCTT GTGCA); GAPDH reverse (TTCTCGGCCTTGACTGTGCCG).

Immunofluorochemistry and image analysis. Transfected cells were washed briefly with PBS containing Ca^{2+} and Mg^{2+} (Mediatech), and fixed with 4% paraformaldehyde (EMS) at room temperature for 20 minutes. Cells were then incubated for 2 hours at room temperature in blocking buffer containing 0.2% Triton X-100, 3% wt/vol BSA, 10% goat serum (Sigma-Aldrich), and combinations of the following primary antibodies with rabbit anti-Tuj1 (Covance, Princeton, NJ; 1:500): mouse anti-MAP2 (Sigma-Aldrich, 1:500), mouse anti-synaptophysin (BD, 1:100), or mouse anti-Tau (BD, 1:50). The cells were then washed three times with PBS, and incubated for 1 hour at room temperature in blocking buffer containing Alexa Fluor 488 goat anti-mouse IgG and Alexa Fluor 594 goat anti-rabbit IgG (Invitrogen), washed three times with PBS, and imaged with a Nikon Eclipse TE2000-U inverted fluorescence microscope (Nikon, Tokyo, Japan) with a ProScanII motorized stage (Prior Scientific, Rockland, MA).

To quantify the relationship between $Tuj1^+$ cell generation and the number of serial BAM factor transfections, PMEFs were transfected in TCPS wells, stained for Tuj1, and scanned to produce large mosaic images of each complete culture area. These mosaics were processed with a FIJI (Fiji Is Just ImageJ, http://fiji.sc) macro to: automatically and uniformly threshold each image according to local contrast, exclude small debris, and to count the number of $Tuj1^+$ cells in each well. These counts were then divided by the number of PMEFs seeded in each well to calculate % $Tuj1^+$ cell generation efficiencies.

Electrophysiology. NiNs cultured on poly-D-lysine/laminin-coated glass coverslips (BD) were identified for patch clamp analysis by synapsin promoter-driven RFP expression[34] after 12–17 days of culture in N3 medium. One dose of p(CBA-ABOL)/BAM factors produced synapsin-RFP^+ cells that were too sparse to find readily with the patch clamping apparatus, and five doses kept unconverted PMEFs in serum-containing medium for an additional 4 days compared to three doses, allowing a layer of cells to develop on the back of the coverslips, which made it more difficult to affix samples securely to our patching setup. So, we elected to patch cells that received three doses. Micropipettes had resistances between 3–7 MΩ, and were filled with internal solution containing: 130 mmol/l $KMeSO_3$, 10 mmol/l HEPES, 10 mmol/l sodium phosphocreatine, 4 mmol/l $MgCl_2$, 4 mmol/l Na_2ATP, 0.4 mmol/l Na_2GTP, 3 mmol/l sodium L-ascorbic acid, with pH 7.24 and an osmolarity of 290 mmol/l. The cells were perfused with artificial cerebral spinal fluid saturated with 5% O_2 and 95% CO_2 and containing: 130 mmol/l NaCl, 2.5 mmol/l KCl, 2 mmol/l $NaHCO_3$, 1.25 mmol/l NaH_2PO_4, 25 mmol/l glucose, 2 mmol/l $CaCl_2$, and 2 mmol/l $MgCl_2$. Gigaohm membrane seals were formed under voltage-clamp conditions. Action potentials were then recorded using an Axon Multiclamp 700B Microelectrode Amplifier (Molecular Devices, Sunnyvale, CA) by stepwise whole-cell current clamp injections, and analyzed with custom in-house MATLAB programs.

Acknowledgments. This work is supported by National Science Foundation EEC-0425626, National Institutes of Health (NIH) EB015300, NIH HL89764, the American Heart Association (C.L.G.), a BD Biosciences Immunology Research grant (C.L.G.), the Swiss National Science Foundation grant PA00P3_124163, and the Howard Hughes Medical Institute (R.Y.). We thank Chai Hoon Quek (Duke University, Durham, NC) for NMR characterization of p(CBA-ABOL) and Nicolas Christoforou (Duke University, Durham, NC) for helpful scientific discussion. We are also grateful for the generous gifts of the Tet-O-FUW-Brn2, Tet-O-FUW-Ascl1, and Tet-O-FUW-Myt1l plasmids from Marius Wernig (Stanford University School of Medicine, Stanford, CA), as well as the psPAX2 and pMD2.G plasmids from Didier Trono (Ecole Polytechnique Fédérale de Lausanne (EPFL), Lausanne, Switzerland), and pLV-hSyn-RFP from Edward M Callaway (The Salk Institute for Biological Sciences, La Jolla, CA). The authors declared no conflict of interest.

1. Han, SS, Williams, LA and Eggan, KC (2011). Constructing and deconstructing stem cell models of neurological disease. *Neuron* **70**: 626–644.
2. Urbaniak Hunter, K, Yarbrough, C and Ciacci, J (2010). Gene- and cell-based approaches for neurodegenerative disease. *Adv Exp Med Biol* **671**: 117–130.
3. Korecka, JA, Verhaagen, J and Hol, EM (2007). Cell-replacement and gene-therapy strategies for Parkinson's and Alzheimer's disease. *Regen Med* **2**: 425–446.
4. Freed, CR, Greene, PE, Breeze, RE, Tsai, WY, DuMouchel, W, Kao, R et al. (2001). Transplantation of embryonic dopamine neurons for severe Parkinson's disease. *N Engl J Med* **344**: 710–719.
5. Mendez, I, Dagher, A, Hong, M, Gaudet, P, Weerasinghe, S, McAlister, V et al. (2002). Simultaneous intrastriatal and intranigral fetal dopaminergic grafts in patients with Parkinson disease: a pilot study. Report of three cases. *J Neurosurg* **96**: 589–596.
6. Peschanski, M, Defer, G, N'Guyen, JP, Ricolfi, F, Monfort, JC, Remy, P *et al.* (1994). Bilateral motor improvement and alteration of L-dopa effect in two patients with Parkinson's disease following intrastriatal transplantation of foetal ventral mesencephalon. *Brain* **117** (Pt 3): 487–499.
7. Lindvall, O, Brundin, P, Widner, H, Rehncrona, S, Gustavii, B, Frackowiak, R *et al.* (1990). Grafts of fetal dopamine neurons survive and improve motor function in Parkinson's disease. *Science* **247**: 574–577.
8. Astradsson, A, Cooper, O, Vinuela, A and Isacson, O (2008). Recent advances in cell-based therapy for Parkinson disease. *Neurosurg Focus* **24**: E6.
9. Olanow, CW, Goetz, CG, Kordower, JH, Stoessl, AJ, Sossi, V, Brin, MF *et al.* (2003). A double-blind controlled trial of bilateral fetal nigral transplantation in Parkinson's disease. *Ann Neurol* **54**: 403–414.
10. Bjorklund, LM, Sánchez-Pernaute, R, Chung, S, Andersson, T, Chen, IY, McNaught, KS *et al.* (2002). Embryonic stem cells develop into functional dopaminergic neurons after transplantation in a Parkinson rat model. *Proc Natl Acad Sci USA* **99**: 2344–2349.
11. Okita, K, Ichisaka, T and Yamanaka, S (2007). Generation of germline-competent induced pluripotent stem cells. *Nature* **448**: 313–317.
12. Wernig, M, Zhao, JP, Pruszak, J, Hedlund, E, Fu, D, Soldner, F *et al.* (2008). Neurons derived from reprogrammed fibroblasts functionally integrate into the fetal brain and improve symptoms of rats with Parkinson's disease. *Proc Natl Acad Sci USA* **105**: 5856–5861.
13. Vierbuchen, T, Ostermeier, A, Pang, ZP, Kokubu, Y, Südhof, TC and Wernig, M (2010). Direct conversion of fibroblasts to functional neurons by defined factors. *Nature* **463**: 1035–1041.
14. Pang, ZP, Yang, N, Vierbuchen, T, Ostermeier, A, Fuentes, DR, Yang, TQ *et al.* (2011). Induction of human neuronal cells by defined transcription factors. *Nature* **476**: 220–223.
15. Pfisterer, U, Kirkeby, A, Torper, O, Wood, J, Nelander, J, Dufour, A *et al.* (2011). Direct conversion of human fibroblasts to dopaminergic neurons. *Proc Natl Acad Sci USA* **108**: 10343–10348.
16. Caiazzo, M, Dell'Anno, MT, Dvoretskova, E, Lazarevic, D, Taverna, S, Leo, D *et al.* (2011). Direct generation of functional dopaminergic neurons from mouse and human fibroblasts. *Nature* **476**: 224–227.
17. Liu, X, Li, F, Stubblefield, EA, Blanchard, B, Richards, TL, Larson, GA *et al.* (2012). Direct reprogramming of human fibroblasts into dopaminergic neuron-like cells. *Cell Res* **22**: 321–332.
18. Kim, J, Su, SC, Wang, H, Cheng, AW, Cassady, JP, Lodato, MA *et al.* (2011). Functional integration of dopaminergic neurons directly converted from mouse fibroblasts. *Cell Stem Cell* **9**: 413–419.
19. Addis, RC, Hsu, FC, Wright, RL, Dichter, MA, Coulter, DA and Gearhart, JD (2011). Efficient conversion of astrocytes to functional midbrain dopaminergic neurons using a single polycistronic vector. *PLoS ONE* **6**: e28719.
20. Son, EY, Ichida, JK, Wainger, BJ, Toma, JS, Rafuse, VF, Woolf, CJ *et al.* (2011). Conversion of mouse and human fibroblasts into functional spinal motor neurons. *Cell Stem Cell* **9**: 205–218.
21. Qiang, L, Fujita, R, Yamashita, T, Angulo, S, Rhinn, H, Rhee, D *et al.* (2011). Directed conversion of Alzheimer's disease patient skin fibroblasts into functional neurons. *Cell* **146**: 359–371.
22. Marro, S, Pang, ZP, Yang, N, Tsai, MC, Qu, K, Chang, HY *et al.* (2011). Direct lineage conversion of terminally differentiated hepatocytes to functional neurons. *Cell Stem Cell* **9**: 374–382.
23. Ambasudhan, R, Talantova, M, Coleman, R, Yuan, X, Zhu, S, Lipton, SA *et al.* (2011). Direct reprogramming of adult human fibroblasts to functional neurons under defined conditions. *Cell Stem Cell* **9**: 113–118.
24. Yoo, AS, Sun, AX, Li, L, Shcheglovitov, A, Portmann, T, Li, Y *et al.* (2011). MicroRNA-mediated conversion of human fibroblasts to neurons. *Nature* **476**: 228–231.
25. Biasco, L, Baricordi, C and Aiuti, A (2012). Retroviral integrations in gene therapy trials. *Mol Ther* **20**: 709–716.
26. Montserrat, N, Garreta, E, González, F, Gutiérrez, J, Eguizábal, C, Ramos, V *et al.* (2011). Simple generation of human induced pluripotent stem cells using poly-beta-amino esters as the non-viral gene delivery system. *J Biol Chem* **286**: 12417–12428.
27. Lee, CH, Kim, JH, Lee, HJ, Jeon, K, Lim, H, Choi, H *et al.* (2011). The generation of iPS cells using non-viral magnetic nanoparticle based transfection. *Biomaterials* **32**: 6683–6691.
28. Okita, K, Nakagawa, M, Hyenjong, H, Ichisaka, T and Yamanaka, S (2008). Generation of mouse induced pluripotent stem cells without viral vectors. *Science* **322**: 949–953.
29. Jia, F, Wilson, KD, Sun, N, Gupta, DM, Huang, M, Li, Z *et al.* (2010). A nonviral minicircle vector for deriving human iPS cells. *Nat Methods* **7**: 197–199.
30. Gonzalez, F, Barragan Monasterio, M, Tiscornia, G, Montserrat Pulido, N, Vassena, R, Batlle Morera, L *et al.* (2009). Generation of mouse-induced pluripotent stem cells by transient expression of a single nonviral polycistronic vector. *Proc Natl Acad Sci USA* **106**: 8918–8922.
31. Wheeler, DG and Cooper, E (2001). Depolarization strongly induces human cytomegalovirus major immediate-early promoter/enhancer activity in neurons. *J Biol Chem* **276**: 31978–31985.
32. Kügler, S, Kilic, E and Bähr, M (2003). Human synapsin 1 gene promoter confers highly neuron-specific long-term transgene expression from an adenoviral vector in the adult rat brain depending on the transduced area. *Gene Ther* **10**: 337–347.
33. Hioki, H, Kameda, H, Nakamura, H, Okunomiya, T, Ohira, K, Nakamura, K *et al.* (2007). Efficient gene transduction of neurons by lentivirus with enhanced neuron-specific promoters. *Gene Ther* **14**: 872–882.
34. Nathanson, JL, Yanagawa, Y, Obata, K and Callaway, EM (2009). Preferential labeling of inhibitory and excitatory cortical neurons by endogenous tropism of adeno-associated virus and lentivirus vectors. *Neuroscience* **161**: 441–450.
35. Jordan, M and Wurm, FM (2003). *Co-transfer of multiple plasmids/viruses as an attractive method to introduce several genes in mammalian cells*. In: Makrides, SC (ed.). New Comprehensive Biochemistry, **vol. 38**. Elsevier: Amsterdam, Netherlands. pp. 337–348.
36. Lin, C, Zhong, Z, Lok, MC, Jiang, X, Hennink, WE, Feijen, J *et al.* (2007). Novel bioreducible poly(amido amine)s for highly efficient gene delivery. *Bioconjug Chem* **18**: 138–145.
37. Vierbuchen, T and Wernig, M (2011). Direct lineage conversions: unnatural but useful? *Nat Biotechnol* **29**: 892–907.
38. Yang, N, Ng, YH, Pang, ZP, Südhof, TC and Wernig, M (2011). Induced neuronal cells: how to make and define a neuron. *Cell Stem Cell* **9**: 517–525.
39. Citri, A, Pang, ZP, Südhof, TC, Wernig, M and Malenka, RC (2012). Comprehensive qPCR profiling of gene expression in single neuronal cells. *Nat Protoc* **7**: 118–127.
40. Kaji, K, Norrby, K, Paca, A, Mileikovsky, M, Mohseni, P and Woltjen, K (2009). Virus-free induction of pluripotency and subsequent excision of reprogramming factors. *Nature* **458**: 771–775.
41. Lauret, E and Baserga, R (1988). Inhibition of gene expression at the translational level by cotransfection with competitor plasmids. *DNA* **7**: 151–156.
42. Ladewig, J, Mertens, J, Kesavan, J, Doerr, J, Poppe, D, Glaue, F *et al.* (2012). Small molecules enable highly efficient neuronal conversion of human fibroblasts. *Nat Methods* 9: 575–578.
43. Rodnitzky, RL (2012). Upcoming treatments in Parkinson's disease, including gene therapy. *Parkinsonism Relat Disord* **18** (suppl. 1): S37–S40.
44. Feng, R, Desbordes, SC, Xie, H, Tillo, ES, Pixley, F, Stanley, ER *et al.* (2008). PU.1 and C/EBPalpha/beta convert fibroblasts into macrophage-like cells. *Proc Natl Acad Sci USA* **105**: 6057–6062.
45. Kajimura, S, Seale, P, Kubota, K, Lunsford, E, Frangioni, JV, Gygi, SP *et al.* (2009). Initiation of myoblast to brown fat switch by a PRDM16-C/EBP-beta transcriptional complex. *Nature* **460**: 1154–1158.
46. Ieda, M, Fu, JD, Delgado-Olguin, P, Vedantham, V, Hayashi, Y, Bruneau, BG *et al.* (2010). Direct reprogramming of fibroblasts into functional cardiomyocytes by defined factors. *Cell* **142**: 375–386.
47. Sekiya, S and Suzuki, A (2011). Direct conversion of mouse fibroblasts to hepatocyte-like cells by defined factors. *Nature* **475**: 390–393.
48. Huang, P, He, Z, Ji, S, Sun, H, Xiang, D, Liu, C *et al.* (2011). Induction of functional hepatocyte-like cells from mouse fibroblasts by defined factors. *Nature* **475**: 386–389.

Supplementary Information accompanies this paper on the Molecular Therapy–Nucleic Acids website (http://www.nature.com/mtna)